



Base- or acid-assisted polystyrene plastic degradation in supercritical CO₂

Yanbing Liu¹ · Jinwen Shi¹ · Liuhao Mao¹ · Bingru Lu¹ · Xing Kang¹ · Hui Jin¹

Received: 14 November 2022 / Revised: 23 January 2023 / Accepted: 20 February 2023 / Published online: 18 March 2023
© Zhejiang University Press 2023

Abstract

Plastic has caused serious "white pollution" to the environment, and the highly inert characteristics of plastic bring a major challenge for degradation. Supercritical fluids have unique physical properties and have been widely used in various fields. In this work, supercritical CO₂ (Sc-CO₂) with mild conditions was selected and assisted by NaOH/HCl solution to degrade polystyrene (PS) plastic, and the reaction model was designed using response surface methodology (RSM). It was found that, regardless of the types of assistance solutions, the factors affecting PS degradation efficiencies were reaction temperature, reaction time, and NaOH/HCl concentration. At the temperature of 400 °C, time of 120 min, and base/acid concentration of 5% (in weight), 0.15 g PS produced 126.88/116.99±5 mL of gases with 74.18/62.78±5 mL of H₂, and consumed 81.2/71.5±5 mL of CO₂. Sc-CO₂ created a homogeneous environment, which made PS highly dispersed and uniformly heated, thus promoting the degradation of PS. Moreover, Sc-CO₂ also reacted with the degradation products to produce new CO and more CH₄ and C₂H_x (x=4, 6). Adding NaOH/HCl solution not only improved the solubility of PS in Sc-CO₂, but also provided a base/acid environment that reduced the activation energy of the reaction, and effectively improved the degradation efficiencies of PS. In short, degrading PS in Sc-CO₂ is feasible, and better results are obtained with the assistance of base/acid solution, which can provide a reference for the disposal of waste plastics in the future.

Keywords Plastic degradation · Polystyrene · Supercritical CO₂ · NaOH · HCl

Introduction

Plastics are widely used because of their outstanding advantages, such as light weight, good ductility, durability, low cost, and ease of processing [1, 2]. The replacement of traditional manufacturing materials by plastics, the dramatic increase in world population, and accessibility to a consumer society are the main reasons for the increasing use of plastic material [3, 4]. Although plastic products have played an important role in protecting people since the outbreak of the COVID-19 epidemic, up to 1.6 million tons of plastic waste are generated every day worldwide [5, 6]. Only about 2% of

world plastics are recycled, and the majority (about 92%) are disposed of in landfills or in the natural environment [3, 4]. Plastics need about 200–400 years to be completely degraded in the natural environment due to their highly inert chemical characteristics [7, 8]. Waste plastic in the environment not only causes visual "white pollution" but also destroys the ecological environment, and therefore threatens the animals, plants, microorganisms, and even humans [9, 10].

Among the methods of handling waste plastics, the most widely used is landfill disposal together with disposal of other wastes [11, 12]. Although this method is simple to operate and the initial investment cost is low, it causes secondary pollution to the land and wastes land resources, and even the CH₄ and other gases produced after landfill are prone to explosion [13, 14]. Incineration is also a common method of disposing waste plastics [15, 16]. In contrast to the landfill method, incineration has the advantages of a short handling cycle, high efficiency, and small footprint. Besides, the large amount of heat energy released by incineration can be used secondarily for power generation and

✉ Jinwen Shi
jinwen_shi@mail.xjtu.edu.cn

✉ Hui Jin
jinhui@mail.xjtu.edu.cn

¹ International Research Center for Renewable Energy, State Key Laboratory of Multiphase Flow in Power Engineering, Xi'an Jiaotong University, 28 West Xianning Road, Xi'an 710049, Shaanxi, China

heating [17, 18]. However, burning plastics produces smoke, solid particles and other substances that are harmful to the environment and humans [19, 20]. In addition, the recycling and reuse of plastics has been a hot topic of research in recent years [21, 22]. With this method, the recycled plastic is processed and turned into valuable substances, effectively improving resource utilization [23, 24].

Supercritical technology to degrade plastics is attracting the attention of researchers [25, 26]. Cheng et al. [27] studied the degradation behavior of carbon fiber reinforced plastics (CFRP) in supercritical alcohols and acetone, and developed a kinetic model for the degradation reaction rate. Different supercritical fluids showed the reaction rate constants for CFRP degradation in the following order: $k_{n\text{-butanol}} > k_{\text{acetone}} > k_{\text{ethanol}} > k_{n\text{-propanol}} > k_{\text{isopropanol}} > k_{\text{methanol}}$. Degradation efficiency of CFRP increased from 78.38% to 94.45% in supercritical n-butanol at 320 °C for 30 min to 240 min. Bai et al. [28] investigated the effects of temperature (500–800 °C), time (1–60 min), pressure (22–25 MPa) and feedstock concentration (2%–10%, in weight) on gasification characteristics of high impact polystyrene (HIPS) plastic in supercritical water. Gasification efficiency of plastic could be improved by increasing the reaction temperature, time, and decreasing the feedstock concentration, but the variation in pressure had little effect. Under the optimal operating conditions (temperature of 800 °C, time of 60 min, pressure of 23 MPa, and feedstock concentration of 3% in weight), plastic carbon conversion reached 94.48%. No auxiliaries or catalysts were added in these studies, so the reaction conditions were relatively harsh, such as higher temperatures and pressures.

Adding auxiliaries or catalysts that can make the reaction or degradation conditions mild has been a hot topic of study in recent years. Onwudili and Williams [29] investigated the catalytic supercritical water gasification (SWG) of olefin plastics (polystyrene: PS, low density polyethylene: LDPE, high density polyethylene: HDPE, and polypropylene: PP) in the presence of RuO₂/Al₂O₃ catalysts to produce CH₄. The highest amount of CH₄ produced from LDPE was 37 mol/kg at 450 °C for 60 min. Catalysis mechanisms involved in the gasification of plastics include steam reforming, water–gas shift reaction (WGS) and methanation. CH₄, H₂ and CO₂ were produced at high temperature from the plastics, and these gases were converted to more CO and H₂ by steam reforming, and RuO₂ was reduced to Ru metal. Subsequently, CO was reacted with water via WGS to produce CO₂ and more H₂. Steam reforming and WGS occurred almost simultaneously. Finally, CO₂ and H₂ were catalyzed by Ru metal to produce CH₄. Okajima and Sako [30] evaluated the effect of different catalysts (K₂CO₃, Na₂CO₃, KOH and NaOH) in subcritical water on recovered carbon fibers from plastics. All four catalysts showed significant catalytic effects,

and among them, K₂CO₃ was the optimal catalyst with a maximum yield up to 71% of phenolic monomer at 400 °C, 20 MPa, 45 min. Carbonate catalysts had higher activity than hydroxide catalysts, and potassium catalysts had better activity than sodium catalysts.

In the presence of catalysts, it was obvious that the degradation effect of plastics was improved, but the catalysts were easily oxidized or reduced in supercritical fluids. Besides, currently, the main supercritical fluids used to recycle plastics are water, alcohols and ketones [31]. These reaction media not only require high temperature and pressure to reach the supercritical state but are also difficult to remove from the reactor after the reaction because they are liquid at room temperature and pressure [32, 33]. In comparison, supercritical CO₂ (Sc-CO₂) has milder conditions (critical pressure of 7.29 MPa and critical temperature of 31.26 °C), and it is easily removed with less residue, as CO₂ is gas at ambient temperature and pressure. Besides, Sc-CO₂ can also thermochemically reduce CO₂ or fix CO₂ for emission reduction [34, 35]. Applications of Sc-CO₂ in different fields have been widely explored, such as the preparation of nanosheet [36], extraction of oil [37], degradation of coal [38], and recycling of power generation [39]. Wei et al. [40] prepared carbon microspheres by converting polyethylene terephthalate (PET) in Sc-CO₂ for use in lithium-ion battery anode material. The yield of carbon microspheres was as high as 47.5% at 650 °C for 9 h. Sc-CO₂ facilitated the decomposition of PET into aromatic hydrocarbon, which further decomposed to produce carbon microspheres. Our group [41] studied the carbon gasification process of PS in supercritical H₂O/CO₂. The presence of CO₂ increased the carbon conversion efficiency (CE) of the PS, reaching 47.6% of CE at 20 min, 700 °C, and 12.5% of consumed CO₂.

Although the application of Sc-CO₂ has been very widespread, there are almost no studies on the degradation of plastics in Sc-CO₂ [42, 43]. Therefore, in the current work, an approach for the degradation of PS plastics in Sc-CO₂ was proposed. Supercritical CO₂ not only provided a homogeneous environment for the degradation process of plastics, but also acted as a solvent that reduced the mass transfer resistance between material interfaces [40]. There is also a unique advantage of using Sc-CO₂, i.e., after the reaction, CO₂ can be completely released as gas at ambient temperature and pressure without affecting the separation of products. Moreover, the solubility of feedstocks in Sc-CO₂ is limited and is usually improved by the addition of co-solvents [44]. Thereby, in this work, a base or acid solution was added to Sc-CO₂ to assist PS degradation. Besides, the reaction models were designed using response surface methodology (RSM) to explore the effects of different factors on the experimental results and the interactions between the factors. Finally, the degradation results and products under different conditions were analyzed as a reference for degrading

plastics or recovering resources from waste plastics in the future.

Feedstocks and methods

Feedstocks

PS plastic powder was used as the experimental feedstock, and the molecular structure is shown in Fig. S1 (Supplementary Information). Detailed information about the elemental analysis, proximate analysis, and gasification characteristics of PS sample are given in Table S1 and Fig. S2 (Supplementary Information). It was found from the molecular structure and elemental analysis that PS is mainly composed of C and H elements with a content of 98.43% (in weight) and a small amount of O and N. From the gasification results of PS, whether in N₂ or CO₂ atmosphere, the initial gasification temperature of PS was about 350 °C, and the weight loss reached 100% at about 450 °C. In contrast to N₂ atmosphere, CO₂ atmosphere could advance the weight loss of PS by about 2 °C.

Methods

All experiments were carried out in a reactor (1 cm inner diameter×15 cm length) made of iron-nickel alloy that could withstand a pressure and temperature of 30 MPa and 800 °C, respectively [41]. Figure 1 shows a schematic diagram of PS plastic degradation in Sc-CO₂. PS (0.15 g) and 1 mL base/acid solution were added before each experiment, and the reactor was purged with CO₂. A certain amount of CO₂ was added before the start of the reaction to maintain the initial pressure of the reactor at 6 MPa. Reactor was set on a heating furnace, the pressure of the reactor increased with the temperature, and the timing was started when the

pressure shown on the monitor rose to 7.29 MPa (critical pressure of CO₂). Reaction temperature (300–500 °C), time (30–120 min) and concentration of the base/acid solution (1%–5%, in weight) were varied, and the products were collected after reactions. Gases were collected completely at the outlet of the reactor using a 3 L aluminum foil sampling bag (E-Switch, Shanghai Shen Yuan Scientific Instruments Co., Ltd., Shanghai, China), followed by opening the reactor and collecting liquids and solid residues with several washes of CH₂Cl₂. Both liquids and solid residues were obtained separately by centrifugation and dried in an oven for 10 h.

To investigate the effects of single or multiple factors on the experimental results, the effects of reaction temperature, reaction time and base/acid solution concentration on the results of PS degradation in Sc-CO₂ were studied using the RSM. Box-Behnken design (BBD) gave 17 experiments (Table S2 in Supplementary Information), evaluated the experimental data, and generated response surface. The experimental results were fitted to a second-order polynomial equation, the accuracy of the model was predicted using statistical analysis of variance (ANOVA), and single- and multi-factor interactions were given to optimize the response conditions.

Product analysis

Plastic degradation efficiency (Y) was calculated using Eq. 1. Products obtained from the degradation of PS in Sc-CO₂ included gases, liquids and solid residues, and these products were analyzed using different methods. The components of gases products were analyzed using gas chromatograph (GC, Agilent 7890, Agilent Technologies, Santa Clara, CA, USA). Solid residues were analyzed by scanning electron microscope (SEM, Superscan SSX-550, Kyoto, Japan) and energy dispersive X-ray spectroscope (EDS) for their morphologies and elements. Liquid products obtained at the end of reactions were analyzed using a gas chromatograph-mass spectrometer (GC-MS, Agilent 7890, Agilent Technologies, Santa Clara, CA, USA).

$$Y = \frac{m_0}{m} \times 100\% \quad (1)$$

where m is the mass of the initial PS, *i.e.*, 0.15 g; m_0 is the mass of the solid residue after degradation.

Results and discussion

RSM-BBD results

Experiments were designed with the reaction temperature (A), reaction time (B) and base/acid concentration (C) as

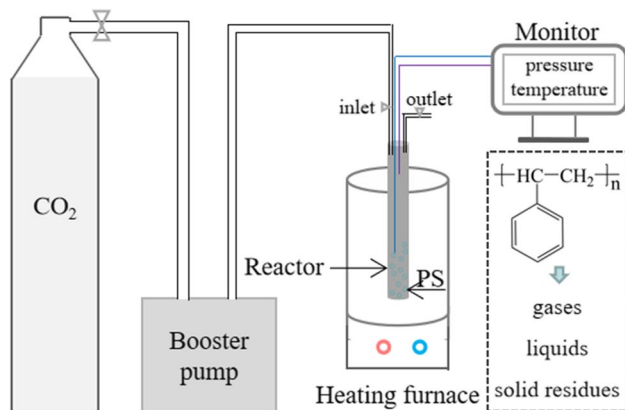


Fig. 1 Schematic diagram of PS plastic degradation in Sc-CO₂. PS polystyrene, Sc-CO₂ supercritical CO₂

independent variables and degradation efficiency (Y) of PS as the response value, and results are shown in Table S2 (Supplementary Information). Quadratic response surface regression analysis was performed on the experimental results to obtain the simulation equations for the degradation efficiency of PS and each independent variable.

$$Y_{\text{NaOH}} = 142.18 - 0.3821A - 0.03102B + 0.6814C \\ + 0.000436AB - 0.001625AC + 0.00603BC \\ + 0.000512A^2 - 0.000398B^2 + 0.00994C^2$$

$$Y_{\text{HCl}} = 119.18 - 0.2682A + 0.00412B + 1.5029C \\ + 0.000102AB - 0.004575AC + 0.014BC \\ + 0.000411A^2 + 0.000073B^2 + 0.038688C^2$$

Table 1 gives the significance tests and ANOVAs for the two regression models. F value means the significance of fitted equation and p -value is used to measure the difference between the predicted and experimental groups. Generally, large F value and low p value ($p < 0.05$) indicate that regression model is significant. For both models, F values were 26.48 and 16.20, respectively, and p values were less than 0.05, which indicated that the model was highly significant. Coefficients R^2 of the two models were 0.9715 and 0.9542, showing that the actual and predicted values were well fitted [45]. Accordingly, the models were significantly regressed and the equations could accurately represent the relationship between PS degradation efficiency and each factor. It could be concluded from the F -values that the main order of each factor influencing the degradation efficiencies of PS was $A > B > C$. This indicated that temperature was the main factor affecting the degradation of plastics and that the base/

acid concentration had the least effect on the degradation of plastics.

In order to explore the interaction between the factors, F values of interaction between the factors are given in Table S3 (Supplementary Information). Under the condition of adding NaOH solution, the interaction between factors A and B was the most pronounced and the interaction between factor A and C was the weakest. However, under the condition of adding HCl solution, the interaction between factors B and C was the most pronounced, and the interaction between factors A and B was the weakest. The factor interaction response surface plots and contour plots are given in Fig. 2. As shown in Fig. 2, the degradation efficiencies of PS increased with each factor regardless of adding NaOH or HCl solution, which was also consistent with the optimized results of RSM-BBD. Optimal conditions for PS degradation were a temperature of 500 °C, time of 120 min, and NaOH/HCl concentration of 5% (in weight), and PS degradation efficiencies could reach almost $100\% \pm 0.05\%$. Experiments were conducted under optimal condition. Degradation efficiency of PS was $99.25\% \pm 0.05\%$ with addition of NaOH solution, which differed from the predicted value by $0.25\% \pm 0.05\%$. Degradation efficiency of PS was $99.88\% \pm 0.05\%$ with addition of HCl solution, which differed from the predicted value by $0.12\% \pm 0.05\%$. Accordingly, the experimental results and the predicted values were similar, indicating that the model was reliable.

Effect of different factors on PS degradation

From the RSM-BBD model, it was found that temperature had the greatest effect on plastic degradation, and the

Table 1 Significance tests and ANOVAs of the regression models

Source	Sum of squares	Degree of freedom	Mean square	F value	P value	
NaOH solution						
Model	548.22	9	60.91	26.48	0.0001	Significant
A	242.66	1	242.66	105.48	<0.0001	
B	167.35	1	167.35	72.74	<0.0001	
C	9.44	1	9.44	4.10	0.0824	
Lack of Fit	10.99	3	3.66	2.86	0.1679	Not significant
$R^2 = 0.9715$						
HCl solution						
Model	506.22	9	56.25	16.20	0.0007	Significant
A	239.48	1	239.48	68.99	<0.0001	
B	154.62	1	154.62	44.54	0.0003	
C	29.18	1	29.18	8.41	0.0230	
Lack of Fit	20.17	3	6.72	6.52	0.0509	Not significant
$R^2 = 0.9542$						

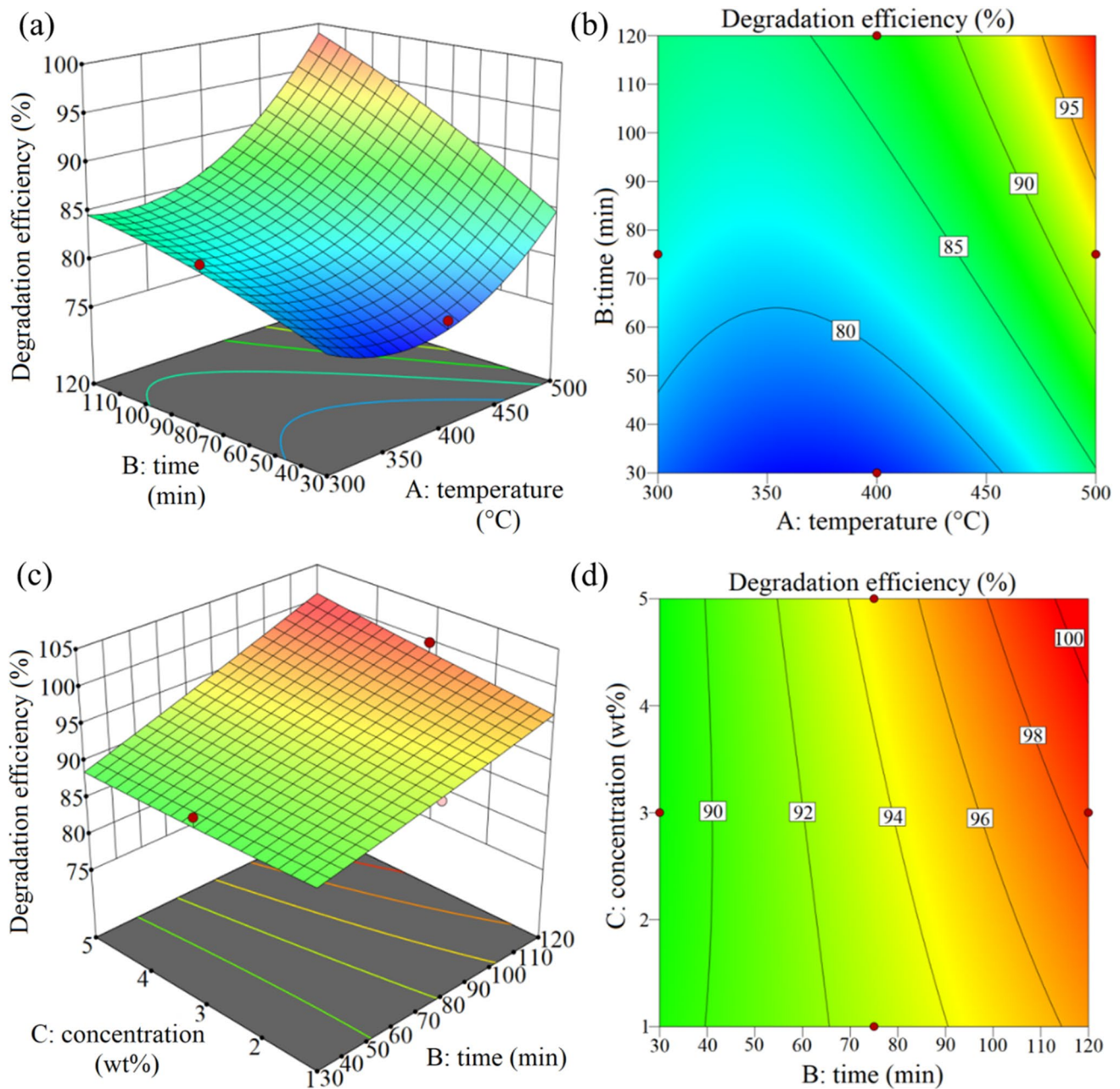


Fig. 2 a, c Response surface plots and b, d contour plots of interaction between factors of reaction temperature (A), reaction time (B), and NaOH/HCl concentration (C): a, b A–B interaction, under the

condition of adding NaOH solution with a concentration of 5% (in weight); c, d B–C interaction, under the condition of adding HCl solution at a reaction temperature of 500 °C

degradation efficiencies of PS at different temperatures are given in Fig. 3. Under either condition, more PS was degraded as the temperature increased from 300 °C to 500 °C, and PS was almost completely degraded when the temperature was 500 °C. At 300 °C, 400 °C and 500 °C, the degradation efficiencies of PS compared with those only at high temperature (only PS groups in Fig. 3) were significantly increased from $52.84\% \pm 0.05\%$, $75.38\% \pm 0.05\%$ and $97.81\% \pm 0.05\%$ to $53.19\% \pm 0.05\%$, $80.58\% \pm 0.05\%$

and $97.43\% \pm 0.05\%$ (or $60.58\% \pm 0.05\%$, $81.72\% \pm 0.05\%$ and $97.89\% \pm 0.05\%$) by adding NaOH (or HCl) solution, respectively. The introduction of Sc-CO₂ created a homogeneous environment for PS to be highly dispersed, and coupled with the solubilization ability of Sc-CO₂, the degradation efficiencies of PS were increased to $58.35\% \pm 0.05\%$, $79.86\% \pm 0.05\%$ and $98.63\% \pm 0.05\%$, respectively. When NaOH (or HCl) solution and Sc-CO₂ acted together, the degradation efficiencies of PS were obviously increased again,

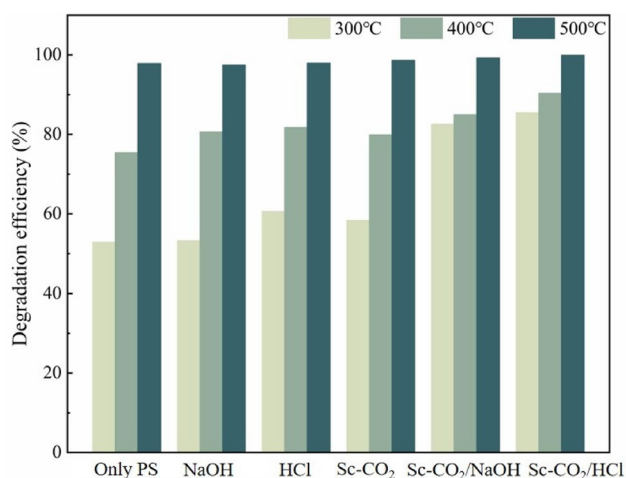


Fig. 3 Effect of reaction temperatures on the degradation efficiencies of PS in different environments (reaction time of 120 min, NaOH/HCl concentration of 5% in weight)

up to $82.53\% \pm 0.05\%$, $84.96\% \pm 0.05\%$ and $99.25\% \pm 0.05\%$ (or $85.42\% \pm 0.05\%$, $90.34\% \pm 0.05\%$ and $99.88\% \pm 0.05\%$) at 300 °C, 400 °C and 500 °C, respectively. It was shown that NaOH/HCl solution and Sc-CO₂ have a synergistic effect on PS degradation, which was attributed to NaOH/HCl solution acting as co-solvent, which improved the solubility of PS in Sc-CO₂ and caused the plastic polymer to swell [46]. In addition, NaOH/HCl also provided OH⁻/H⁺, which created a base/acid environment and reduced the reaction activation energy, accelerating the depolymerization of PS [47].

The effect of reaction time and NaOH/HCl concentration on the PS degradation efficiencies is given in Fig. 4. It was

found that the degradation efficiencies of PS increased over time in both the Sc-CO₂/NaOH and Sc-CO₂/HCl systems, from $77.35\% \pm 0.05\%$ and $81.46\% \pm 0.05\%$ to $86.09\% \pm 0.05\%$ and $92.78\% \pm 0.05\%$, respectively, as the reaction time increased from 30 min to 120 min. Likewise, the degradation efficiencies of PS improved from $82.55\% \pm 0.05\%$ and $84.62\% \pm 0.05\%$ to $86.09\% \pm 0.05\%$ and $92.78\% \pm 0.05\%$, respectively, as the concentration of NaOH/HCl increased from 1% to 5% (in weight). However, different from the results of the temperature effect, the degradation efficiencies of PS showed a moderate increase with time from 30 min to 120 min and NaOH/HCl concentration from 1% to 5% (in weight). It was observed that the degradation of PS was more influenced by the reaction time than by the NaOH/HCl concentration, as shown in Fig. 4a and b. Thus, in combination with Figs. 3 and 4, it could also be found that the reaction temperature had the greatest effect on the degradation of PS, followed by the reaction time and then the NaOH/HCl concentration, which was consistent with the RSM-BBD result.

Products analysis

The products of PS degradation included mixtures of gases, solids (plastic residues) and liquid oils. First, several blank experiments were conducted, i.e., NaOH or HCl solution (concentration of 5%, in weight) interacted with Sc-CO₂ (temperature of 400 °C) without the addition of PS for different times. The results (Table S4 in Supplementary Information) showed that NaOH or HCl solution in Sc-CO₂ produced different amounts of H₂, and corresponding amount of H₂ was subtracted in the subsequent calculation of the

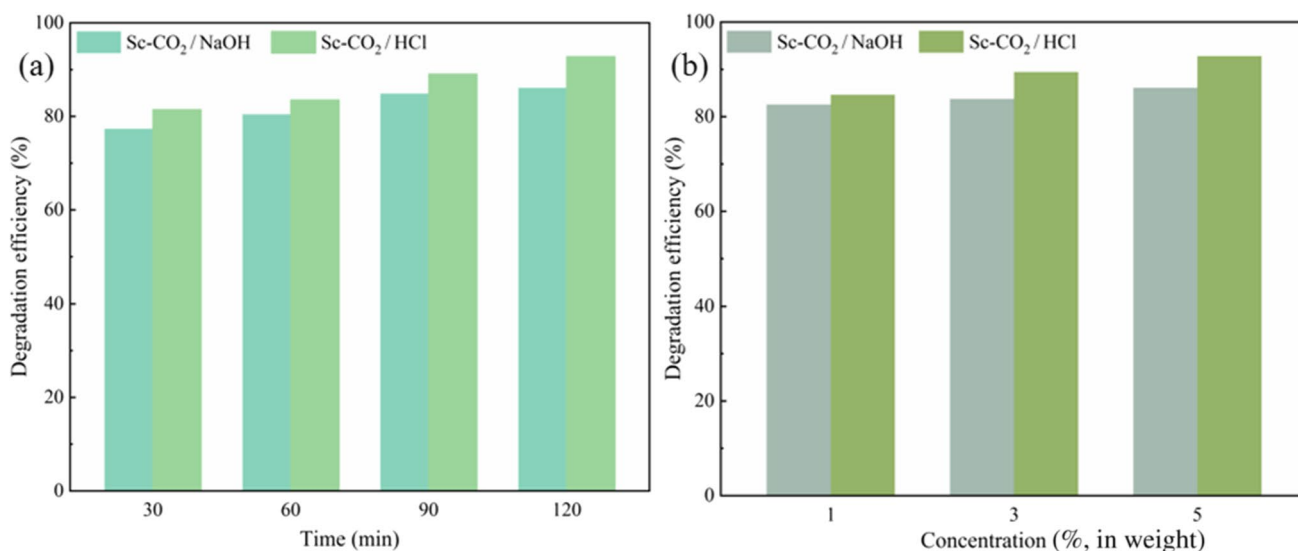


Fig. 4 Effect of **a** reaction time and **b** NaOH/HCl concentration on PS degradation efficiency at a reaction temperature of 400 °C: **a** with an NaOH/HCl concentration of 5 wt%; **b** with a reaction time of 120 min

gases products after PS degradation. The gas products of PS degradation in Sc-CO₂ were H₂, CO, CH₄ and C₂H_x ($x=4, 6$), and their distributions are given in Fig. 5. As could be seen, PS was converted into more gas with a longer reaction time. With a reaction time of 120 min and with the assistance of NaOH/HCl solution, the total gas volume produced by PS degradation reached 126.88/116.99±5 mL, in which the amounts of H₂ and CH₄ were 74.18/62.78±5 mL and 31.68/45.29±5 mL, respectively. The molecular structure and elemental analysis showed that PS was mainly composed of C and H elements. CO₂ not only promoted the degradation of PS in Sc-CO₂, but also reacted with the gas products to produce new CO and more CH₄ and C₂H_x. It was also found that CO₂ consumption increased with the reaction time. With a reaction time of 120 min and with the assistance of NaOH/HCl solution, the consumption of CO₂ was 81.2/71.5±5 mL. More CO₂ was consumed by the reaction with the aid of NaOH solution than HCl solution because a small amount of CO₂ reacted with NaOH to form Na₂CO₃ (Fig. S3 in Supplementary Information), which was verified by the control experiments.

SEM (Everhart–Thornley detector, ETD) was used to analyze the pristine PS plastic and solid residues after PS degradation, as shown in Fig. S4 (Supplementary Information) and Fig. 6, respectively. Also, the elements of the PS residues were analyzed by EDS, and the morphology and corresponding atomic percentages of the residues obtained in different reaction environments were different. Surface of the pristine PS plastic was full of streaks, and with the assistance of NaOH, the residues were mainly microspheres and some scattered flocs. In contrast, with the assistance of HCl, the residues were mainly irregular stripes and trace amounts

of microspheres. It was observed that the residues after PS degradation contained both C and O elements. The Na element was from NaOH solution, and the Cl element was from HCl solution. In addition, Al, Fe and Ni elements were also observed in the residues after HCl treatment, which were not present in the residues after NaOH treatment. It was indicated that the HCl corroded the reactor and made the metal species leaked from the inside of the reactor. Based on the fact that the addition of HCl solution-assisted degradation of PS was more effective, it was speculated that these leaked metal species might play a catalytic role in addition to the effect of HCl itself. To avoid uncertainties caused by the reactor, it can be treated with anticorrosion treatment inside the reactor or use ceramic materials for its better improvement. Compared with HCl, the PS solid residue obtained by NaOH solution-assisted degradation contains more O element. Inferred from the results of the control experiments, this phenomenon should be caused by the production of Na₂CO₃, which also verified that NaOH reacted with CO₂.

The compositions of liquid products after PS degradation mainly consisted of phenanthrene (C₁₄H₁₀), anthracene (C₁₄H₁₀), 1-phenyl-naphthalene (C₁₆H₁₂), 2-phenyl-naphthalene (C₁₆H₁₂), 1-phenylmethyl-naphthalene (C₁₇H₁₄), fluoranthene (C₁₆H₁₀) triphenylene (C₁₈H₁₂) and 1,3,5-triphenylbenzene (C₂₄H₁₈). Figure 7 shows the compositions and relative contents of the liquid products at different reaction temperatures. Detailed retention times and corresponding structures of these substances are given in Table S6 (Supplementary Information). The amount of material peaks in the liquid products decreased as the temperature increased from 300 °C to 500 °C. Combined with the change in the total amount of gas products with reaction temperature, it

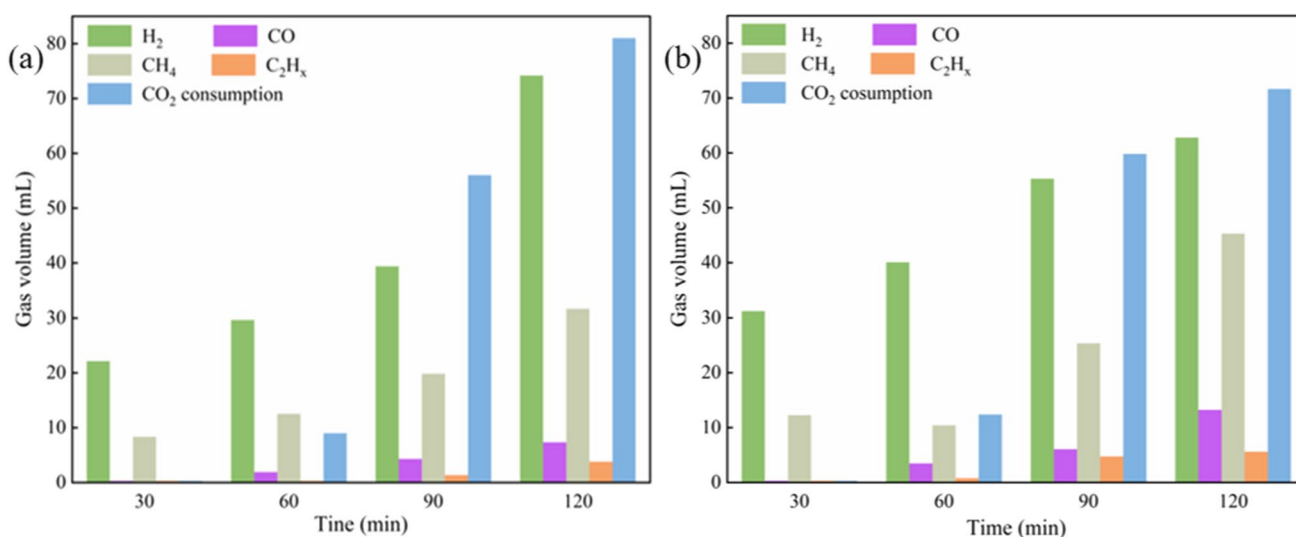


Fig. 5 Gas products of PS degradation assisted by **a** NaOH and **b** HCl solution (NaOH/HCl concentration of 5% in weight, reaction temperature of 400 °C)

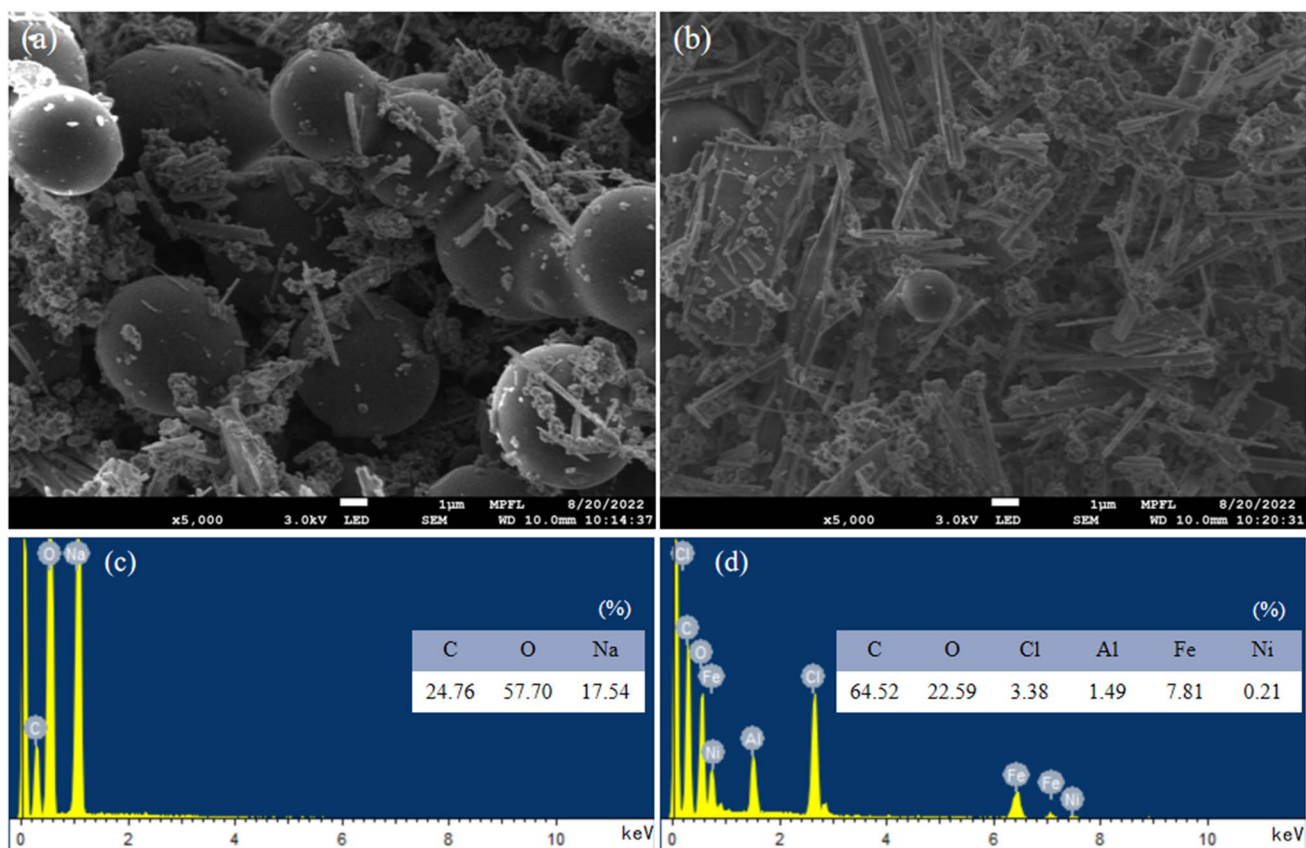


Fig. 6 a, b SEM images and c, d EDS results of solid residues from PS degradation assisted by (a, c) NaOH and (b, d) HCl solution with a concentration of 5% in weight (reaction temperature of 400 °C, reaction time of 120 min). Scale bar: 1 μ m

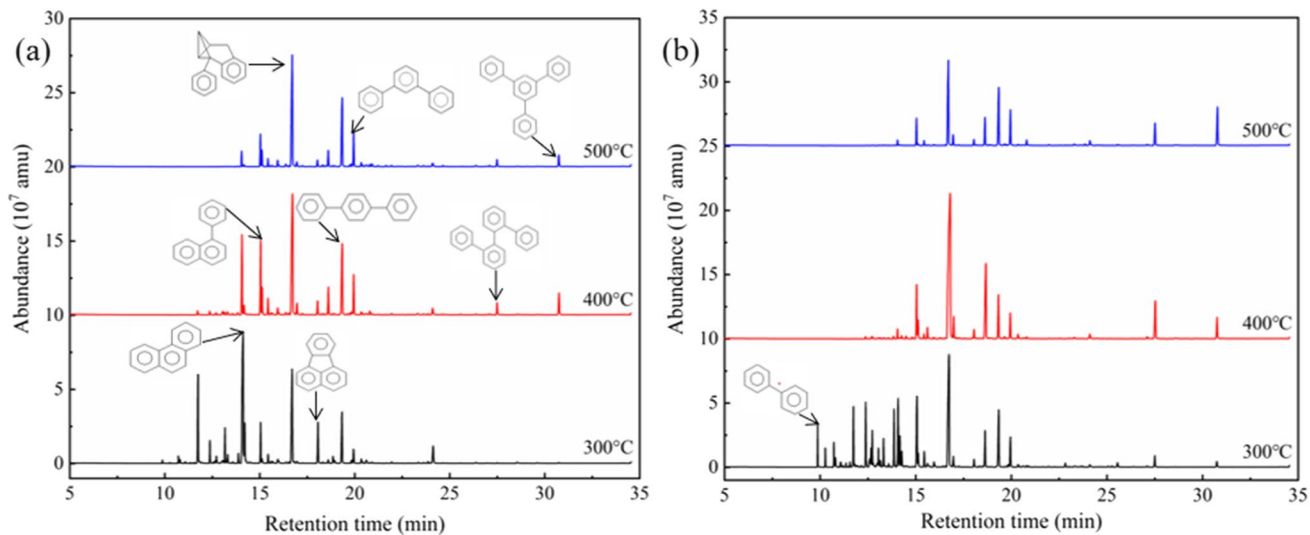
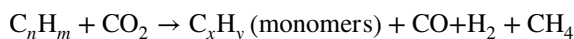
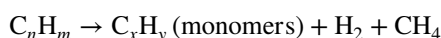
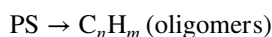


Fig. 7 GC–MS of liquid products from PS degradation at different reaction temperatures assisted by a NaOH and, b HCl solution with a concentration of 5% in weight (reaction time of 120 min). The spec-

tra in (a) were shifted upward by 0, 10×10^7 and 20×10^7 amu, and those in (b) were shifted upward by 0, 10×10^7 and 25×10^7 amu. GC–MS gas chromatograph–mass spectrometer, Amu atomic mass unit

was indicated that more liquid was converted to gas at higher temperature. When the temperature was 300 °C, the liquid products contained more biphenyl, fluorene and benzene, which are commonly used as raw materials for the synthesis of plastics. However, these substances were not observed in the liquid products obtained at 400 and 500 °C. It was indicated that the degradation of PS was more complete at 400 °C and 500 °C than at 300 °C. At higher reaction temperatures, the carbon chain structure of PS undergoes condensation, generating more phenanthrene, 1-phenyl-naphthalene, m-terphenyl, triphenylene and other condensed-ring aromatic substances, which are commonly contained in tar. Moreover, the carbon chain structure of PS was changed, which also promoted the production of more H₂. This result was consistent with the increase in H₂ volume (Table S5 in Supplementary Information) with increasing reaction temperature.

It was thus inferred that a series of reactions occurred during the degradation of PS. PS first decomposed into oligomers and then into monomers, H₂ and CH₄. Oligomers from plastic decomposition and CO₂ reacted to form monomers, H₂, CH₄ and CO. In short, Sc-CO₂ fluid provided a unique degradation environment to effectively improve the degradation efficiencies of PS. More importantly, CO₂ could also react with the products and change the compositions of the products.



Conclusions

In this work, an approach was proposed for the degradation of PS plastics in Sc-CO₂ assisted by NaOH or HCl solution. Reaction models were designed using RSM-BBD to investigate the effects of reaction temperature, reaction time and NaOH/HCl concentration on the degradation of PS, which were verified through experiments. The main conclusions of this work are as follows.

1. RSM-BBD results showed that the effects of a single factor on PS degradation efficiencies were A (reaction temperature) > B (reaction time) > C (NaOH/HCl concentration) in order.
2. At a reaction temperature of 300 °C, reaction time of 120 min, NaOH/HCl concentration of 5% in weight, degradation efficiencies of PS increased significantly from 52.84%±0.05% to 58.35%±0.05%, 82.35%±0.05%

and 85.42%±0.05% with the introduction of Sc-CO₂, Sc-CO₂/NaOH solution and Sc-CO₂/HCl solution, respectively.

3. At a temperature of 400 °C, time of 120 min, and NaOH/HCl concentration of 5% in weight, the PS degradation with an efficiency of 84.96%±0.05%/90.34%±0.05%, produced 126.88/116.99±5 mL of gases with 74.18/62.78±5 mL of H₂, and consumed 81.2/71.5±5 mL of CO₂.
4. With the assistance of NaOH solution, the solid residues after PS degradation were mainly microspheres and some scattered flocs. In contrast, with the assistance of HCl solution, the solid residues were mainly irregular stripes and trace amounts of microspheres.

In the process of PS degradation, Sc-CO₂/NaOH or Sc-CO₂/HCl was introduced to make PS highly dispersed and uniformly heated, and enhanced the solubilization of PS in Sc-CO₂, which promoted more complete degradation of PS. More importantly, CO₂ could react with the products to fix CO₂ and contribute to emission reduction.

Supplementary Information The online version contains supplementary material available at <https://doi.org/10.1007/s42768-023-00139-1>.

Acknowledgements This work was supported by the Basic Science Center Program for Ordered Energy Conversion of the National Natural Science Foundation of China (No.51888103), National Natural Science Foundation of China (No.52242609) and Fundamental Research Funds for the Central Universities.

Data availability The data that support the findings of this study are available from the corresponding author upon reasonable request.

Declarations

Conflict of interest The authors declare no conflict of interest.

References

1. Mansoor, H.S., Alsayed, R., and Abdalh, M. 2021. Polystyrene doped with Schiff base to reduce outdoor plastic degradation for sustainable environment. *South African Journal of Chemical Engineering* 35: 53–59. <https://doi.org/10.1016/j.sajce.2020.11.003>.
2. Sullivan, K.P., Werner, A.Z., Ramirez, K.J., et al. 2022. Mixed plastics waste valorization through tandem chemical oxidation and biological funneling. *Science* 378 (6616): 207–211. <https://doi.org/10.1126/science.abo46>.
3. Kedzierski, M., Frère, D., Le Maguer, G., et al. 2020. Why is there plastic packaging in the natural environment? Understanding the roots of our individual plastic waste management behaviours. *Science of The Total Environment* 740: 139985. <https://doi.org/10.1016/j.scitotenv.2020.139985>.
4. Taghavi, N., Singhal, N., Zhuang, W.Q., et al. 2021. Degradation of plastic waste using stimulated and naturally occurring microbial strains. *Chemosphere* 263: 127975. <https://doi.org/10.1016/j.chemosphere.2020.127975>.

5. Zhao, S., Zhu, B., Bai, B., et al. 2022. Study on carbon fixation and gasification of polypropylene and polycarbonate in a CO₂ environment. *Industrial and Engineering Chemistry Research* 61 (29): 10436–10445. <https://doi.org/10.1021/acs.iecr.2c00178>.
6. Benson, N.U., Bassey, D.E., and Palanisami, T. 2021. COVID pollution: Impact of COVID-19 pandemic on global plastic waste footprint. *Heliyon* 7 (2): e06343–e06343. <https://doi.org/10.1016/j.heliyon.2021.e06343>.
7. Qi, R., Jones, D., Zhen, L., et al. 2019. Behavior of microplastics and plastic film residues in the soil environment: A critical review. *Science of The Total Environment* 703: 134722. <https://doi.org/10.1016/j.scitotenv.2019.134722>.
8. Yang, L., Zhang, Y., Kang, S., et al. 2021. Microplastics in soil: A review on methods, occurrence, sources, and potential risk. *Science of The Total Environment* 780: 146546. <https://doi.org/10.1016/j.scitotenv.2021.146546>.
9. Rillig, M.C., Ziersch, L., and Hempel, S. 2017. Microplastic transport in soil by earthworms. *Scientific Reports* 7 (1): 1362. <https://doi.org/10.1038/s41598-017-01594-7>.
10. Franzellitti, S. 2021. Editorial overview: Plastic pollution and human health: What we know and what we should focus on. *Current Opinion in Toxicology* 28: 84–86. <https://doi.org/10.1016/j.cotox.2021.10.004>.
11. Kumar, R., Pandit, P., Kumar, D., et al. 2021. Landfill microbiome harbour plastic degrading genes: A metagenomic study of solid waste dumping site of Gujarat, India. *Science of The Total Environment* 779: 146184. <https://doi.org/10.1016/j.scitotenv.2021.146184>.
12. Potrykus, M., Redko, V., Głowacka, K., et al. 2021. Polypropylene structure alterations after 5 years of natural degradation in a waste landfill. *Science of The Total Environment* 758: 143649. <https://doi.org/10.1016/j.scitotenv.2020.143649>.
13. Breyer, S., Mekhitarian, L., Rimez, B., et al. 2017. Production of an alternative fuel by the co-pyrolysis of landfill recovered plastic wastes and used lubrication oils. *Waste Management* 60: 363–374. <https://doi.org/10.1016/j.wasman.2016.12.011>.
14. Zhang, Y., Peng, Y., Peng, C., et al. 2021. Comparison of detection methods of microplastics in landfill mineralized refuse and selection of degradation degree indexes. *Environmental Science and Technology* 55 (20): 13802–13811. <https://doi.org/10.1021/acs.est.1c02772>.
15. Shah, N.H., Jayswal, E.N., and Suthar, A.H. 2021. Mathematical modeling on investments in burning and recycling of dumped waste by plastic industry. *International Journal of Environmental Science and Technology* 18 (3): 741–750. <https://doi.org/10.1007/s13762-020-02839-1>.
16. Velis, C.A., and Cook, E. 2021. Mismanagement of plastic waste through open burning with emphasis on the global south: A systematic review of risks to occupational and public health. *Environmental Science and Technology* 55 (11): 7186–7207. <https://doi.org/10.1021/acs.est.0c08536>.
17. Jia, Y., Li, H., and Wang, Z. 2019. Research progress in treatment technology of municipal solid waste in China. *Advances in Environmental Protection* 9: 717–725. <https://doi.org/10.12677/AEP.2019.95095>.
18. Larrain, M., Billen, P., and Van Passel, S. 2022. The effect of plastic packaging recycling policy interventions as a complement to extended producer responsibility schemes: A partial equilibrium model. *Waste Management* 153: 355–366. <https://doi.org/10.1016/j.wasman.2022.09.012>.
19. Verma, R., Vinoda, K.S., Papireddy, M., et al. 2016. Toxic pollutants from plastic waste- A review. *Procedia Environmental Sciences* 35: 701–708. <https://doi.org/10.1016/j.proenv.2016.07.069>.
20. Shen, M., Hu, T., Huang, W., et al. 2021. Can incineration completely eliminate plastic wastes? An investigation of microplastics and heavy metals in the bottom ash and fly ash from an incineration plant. *Science of The Total Environment* 779: 146528. <https://doi.org/10.1016/j.scitotenv.2021.146528>.
21. Adnan, H.M., and Dawood, A.O. 2021. Recycling of plastic box waste in the concrete mixture as a percentage of fine aggregate. *Construction and Building Materials* 284: 122666. <https://doi.org/10.1016/j.conbuildmat.2021.122666>.
22. Chen, H., Wan, K., Zhang, Y., et al. 2021. Waste to wealth: Chemical recycling and chemical upcycling of waste plastics for a great future. *Chemsuschem* 14 (19): 4123–4136. <https://doi.org/10.1002/cssc.202100652>.
23. Lanzalaco, S., Fabregat, G., Muñoz-Galan, H., et al. 2020. Recycled low-density polyethylene for noninvasive glucose monitoring: A proposal for plastic recycling that adds technological value. *ACS Sustainable Chemistry and Engineering* 8 (33): 12554–12560. <https://doi.org/10.1021/acssuschemeng.0c03545>.
24. Xu, X., Leng, Z., Lan, J., et al. 2020. Sustainable practice in pavement engineering through value-added collective recycling of waste plastic and waste tyre rubber. *Engineering* 7 (6): 857–867. <https://doi.org/10.1016/j.eng.2020.08.020>.
25. Lozano-Martinez, P., Torres-Zapata, T., and Martin-Sanchez, N. 2021. Directing depolymerization of PET with subcritical and supercritical ethanol to different monomers through changes in operation conditions. *ACS Sustainable Chemistry and Engineering* 9 (29): 9846–9853. <https://doi.org/10.1021/acssuschemeng.1c02489>.
26. Okajima, I., Watanabe, K., Haramiishi, S., et al. 2016. Recycling of carbon fiber reinforced plastic containing amine-cured epoxy resin using supercritical and subcritical fluids. *Journal of Supercritical Fluids* 119: 44–51. <https://doi.org/10.1016/j.supflu.2016.08.015>.
27. Cheng, H., Huang, H., Liu, Z., et al. 2018. Reaction kinetics of CFRP degradation in supercritical fluids. *Journal of Polymers and the Environment* 26 (5): 2153–2165. <https://doi.org/10.1007/s10924-017-1114-2>.
28. Bai, B., Liu, Y., Wang, Q., et al. 2019. Experimental investigation on gasification characteristics of plastic wastes in supercritical water. *Renewable Energy* 135: 32–40. <https://doi.org/10.1016/j.renene.2018.11.092>.
29. Onwudili, J.A., and Williams, P.T. 2016. Catalytic supercritical water gasification of plastics with supported RuO₂: A potential solution to hydrocarbons–water pollution problem. *Process Safety and Environmental Protection* 102: 140–149. <https://doi.org/10.1016/j.psep.2016.02.009>.
30. Okajima, I., and Sako, T. 2017. Recycling of carbon fiber-reinforced plastic using supercritical and subcritical fluids. *Journal of Material Cycles and Waste Management* 19 (1): 15–20. <https://doi.org/10.1007/s10163-015-0412-9>.
31. Song, Z., Xiu, F., and Qi, Y. 2022. Degradation and partial oxidation of waste plastic express packaging bags in supercritical water: Resources transformation and pollutants removal. *Journal of Hazardous Materials* 423: 127018. <https://doi.org/10.1016/j.jhazmat.2021.127018>.
32. Fan, C., and Jin, H. 2022. A zero-dimensional model of porous char gasification in supercritical water: Experiments and mathematical modeling. *Chemical Engineering Journal* 440: 135954. <https://doi.org/10.1016/j.cej.2022.135954>.
33. Wang, Y., Zhang, M., Wang, H., et al. 2022. The influence of Stefan flow on the flow and heat-transfer characteristics of spherical-particle pair in supercritical water. *International Journal of Multiphase Flow* 151: 104045. <https://doi.org/10.1016/j.ijmul.2022.104045>.
34. Pérez-Mayán, L., Ramil, M., Cela, R., et al. 2021. Supercritical fluid chromatography-mass spectrometric determination of chiral fungicides in viticulture-related samples. *Journal of Chromatography A* 1644: 462124. <https://doi.org/10.1016/j.chroma.2021.462124>.

35. Su, W., Zhang, H., Xing, Y., et al. 2021. A bibliometric analysis and review of supercritical fluids for the synthesis of nanomaterials. *Nanomaterials* 11 (2): 336. <https://doi.org/10.3390/nano11020336>.
36. Tian, X., Li, Y., Chen, Z., et al. 2017. Shear-assisted production of few-layer boron nitride nanosheets by supercritical CO₂ exfoliation and its use for thermally conductive epoxy composites. *Scientific Reports* 7 (1): 17794. <https://doi.org/10.1038/s41598-017-18149-5>.
37. Das, M., Roy, S., Guha, C., et al. 2021. In vitro evaluation of antioxidant and antibacterial properties of supercritical CO₂ extracted essential oil from clove bud (*Syzygium aromaticum*). *Journal of Plant Biochemistry and Biotechnology* 30 (2): 387–391. <https://doi.org/10.1007/s13562-020-00566-9>.
38. Liu, F., Liu, G., Gasem, K.A.M., et al. 2020. Green and efficient two-step degradation approach for converting Powder River Basin coal into fuels/chemicals and insights into their chemical compositions. *Applied Energy* 264: 114739. <https://doi.org/10.1016/j.apenergy.2020.114739>.
39. Jiang, R., Lu, G., Yan, Z., et al. 2021. Microplastic degradation by hydroxy-rich bismuth oxychloride. *Journal of Hazardous Material* 405: 124247. <https://doi.org/10.1016/j.jhazmat.2020.124247>.
40. Wei, L., Yan, N., and Chen, Q. 2021. Converting poly(ethylene terephthalate) waste into carbon microspheres in a supercritical CO₂ system. *Environmental Science and Technology* 45 (2): 534–539. <https://doi.org/10.1021/es102431e>.
41. Zhao, S., Wang, C., Bai, B., et al. 2021. Study on the polystyrene plastic degradation in supercritical water/CO₂ mixed environment and carbon fixation of polystyrene plastic in CO₂ environment. *Journal of Hazardous Materials* 421: 126763. <https://doi.org/10.1016/j.jhazmat.2021.126763>.
42. Elmanovich, I.V., Stakhanov, A.I., Kravchenko, E.I., et al. 2022. Chemical recycling of polyethylene in oxygen-enriched supercritical CO₂. *The Journal of Supercritical Fluids* 181: 105503. <https://doi.org/10.1016/j.supflu.2021.105503>.
43. Elmanovich, I.V., Stakhanov, A.I., Zefirov, V.V., et al. 2020. Thermal oxidation of polypropylene catalyzed by manganese oxide aerogel in oxygen-enriched supercritical carbon dioxide. *The Journal of Supercritical Fluids* 158: 104744. <https://doi.org/10.1016/j.supflu.2019.104744>.
44. Lo, B., Tai, C., Chang, J., et al. 2007. Supercritical carbon dioxide-assisted oxidative degradation and removal of polymer residue after reactive ion etching of photoresist. *Green Chemistry* 9 (2): 133–138. <https://doi.org/10.1039/B602885C>.
45. Zhu, Z., Liu, Y., Cong, W., et al. 2021. Soybean biodiesel production using synergistic CaO/Ag nano catalyst: Process optimization, kinetic study, and economic evaluation. *Industrial Crops and Products* 166: 113479. <https://doi.org/10.1016/j.indcrop.2021.113479>.
46. Ramsden, M., and Phillips, J.A. 1996. Factors influencing the kinetics of the alkaline depolymerisation of poly(ethylene terephthalate). I: The effect of solvent. *Journal of Chemical Technology and Biotechnology* 67: 131–136. [https://doi.org/10.1002/\(SICI\)1097-4660\(199610\)67:2%3c131::AID-JCTB538%3e3.0.CO;2-F](https://doi.org/10.1002/(SICI)1097-4660(199610)67:2%3c131::AID-JCTB538%3e3.0.CO;2-F).
47. Wang, Y., and Zhang, F. 2012. Degradation of brominated flame retardant in computer housing plastic by supercritical fluids. *Journal of Hazardous Materials* 205–206: 156–163. <https://doi.org/10.1016/j.jhazmat.2011.12.055>.

Publisher's Note Springer Nature remains neutral with regard to jurisdictional claims in published maps and institutional affiliations.

Springer Nature or its licensor (e.g. a society or other partner) holds exclusive rights to this article under a publishing agreement with the author(s) or other rightsholder(s); author self-archiving of the accepted manuscript version of this article is solely governed by the terms of such publishing agreement and applicable law.